Available online at www.sciencedirect.com
SCIENCE DIRECT®
International Journal of Thermal Sciences 44 (2005) 255–266
International Journal of Thermal Sciences
www.elsevier.com/locate/ijts

Unsteady ternary mass transfer from a sphere in creeping flow

Gheorghe Juncu

Politehnica University Bucharest, Catedra Inginerie Chimica, Polizu 1, 78126 Bucharest, Romania

Received 19 February 2004; received in revised form 16 August 2004; accepted 16 August 2004

Abstract

The transient mass transfer from a sphere with rigid surface into a surrounding fluid flow has been analysed for a ternary system. The concentrations inside the sphere are considered uniform. Steady, creeping flow is assumed around the sphere. The mass balance equations were solved numerically in spherical coordinates by a finite difference splitting method. The computations focused on the influence of the cross diffusion coefficients on the mass transfer rate at moderate Peclet numbers and different values of the Henry numbers and self-diffusivity rates. The occurrence on the sphere's surface of osmotic diffusion, diffusion barrier and reverse diffusion phenomena was also studied.

Keywords: Ternary mass transfer; Rigid sphere; External problem; Creeping flow

1. Introduction

Prediction of the interfacial mass transfer rate between a sphere and a surrounding fluid is of fundamental importance for a wide range of industrial and scientific applications. Clift et al. [1], Brauer [2], Brounshtein and Shegolev [3] and Sadhal et al. [4] give an extensive coverage of literature about transport phenomena around a sphere. Transport phenomena around a spherical body are usually classified as [1,2]:

- *external problems*, if the sphere may be considered gradientless;
- *internal problems*, if the surrounding phase is gradientless;
- *conjugate problems*, if the transfer resistance in both phases is comparable to each other.

The external and internal problems may be viewed as asymptotic cases of the conjugate problem.

Curtiss and Bird [5] recently observed "a resurgent interest in multicomponent diffusion among workers in separations science, combustion and biological processes". However, the influence of cross diffusion phenomena on the heat/mass transfer from a sphere is the subject of few theoretical and experimental studies. In [1–4] this problem is not even touched.

Theoretically, the multicomponent mass transfer from a sphere was analysed in [6–8]. Negri and Korchinsky [6] solved numerically the multicomponent mass transfer in a spherical rigid drop (the classical internal problem and the quasi-steady-state approximation (QSSA) [9] of the conjugate problem). A thorough investigation of the influence of cross-diffusion coefficients on the mass transfer rate was not made. Only the systems, acetone–methanol–benzene (with negative cross diffusion coefficients) and a fictitious one with positive but very small cross diffusion coefficients, were simulated. Taylor and Krishna [7] proposed a generalization of the Newman and Kronig–Brink models for multicomponent systems.

Based on the boundary layer formalism, Uribe–Ramirez and Korchinsky [8] investigated the multicomponent conjugate mass transfer between a liquid drop and an environmental fluid flow for drop Reynolds numbers in the range 10–250. The mass transfer occurring in the wake was ne-

E-mail addresses: juncu@easynet.ro, juncugh@netscape.net (G. Juncu).
Tel.: +40 21 345 0596, fax: +40 21 345 0596.

1290-0729/$ – see front matter
doi:10.1016/j.ijthermalsci.2004.08.003

Nomenclature

C	mass concentration of the transferring species
d	sphere diameter
$\mathbf{D}$	normalized Fickean diffusion coefficients matrix of the transferring species, $= \mathbf{Đ}/Đ_{11}$
$\mathbf{Đ}$	Fickean diffusion coefficients matrix of the transferring species
$\mathbf{H}$	Henry numbers matrix
$\mathbf{k}$	mass transfer coefficients matrix
Pe	fluid phase Peclet number, $= U_\infty d/Đ_{11}$
r	dimensionless radial coordinate, $2r'/d$, in spherical coordinate system
r'	radial coordinate, spherical coordinate system
$\mathbf{Sh}$	overall instantaneous Sherwood numbers matrix, $Sh_{ij} = k_{ij}d/Đ_{11}$
t	time
U_∞	free-stream fluid velocity
V_R	dimensionless radial velocity component
V_θ	dimensionless tangential velocity component
Z_i	continuous phase dimensionless concentration, $= \frac{C_i - C_{i,\infty}}{C_{di,0}/H_{ii} - C_{i,\infty}}$
Z_{di}	dispersed phase dimensionless concentration, $= \frac{C_{di} - H_{ii}C_{i,\infty}}{C_{di,0} - H_{ii}C_{i,\infty}}$

Greek symbols

γ_{ij}	concentrations ratio, $= \frac{C_{dj,0}/H_{jj} - C_{j,\infty}}{C_{di,0}/H_{ii} - C_{i,\infty}}$
θ	polar angle in spherical coordinate system
τ	dimensionless time or Fourier number, $= 4tĐ_{11}/d^2$

Subscripts

d	dispersed phase
0	initial conditions
∞	large distance from the sphere

glected. A relation to calculate the mass transfer coefficients was derived. The theoretical values were compared with the experimental data of the system toluene–acetone–phenol–water. As in [6], a general analysis concerning the influence of cross-diffusion coefficients on the mass transfer rate was not made.

The general formulation of the multicomponent mass transfer from a sphere is that of a conjugate problem. When the diffusivities inside the sphere are considerably higher than those of continuous phase, the sphere may be considered gradientless (the concentrations inside the sphere are uniform but not constant in time). This way, the conjugate problem reduces to an external problem. The importance of solving the external problem can be argued for in two ways. First, the external problem models quite acceptably enough certain real life cases [2,3,10] (and the references cited herein). Secondly, the external problem is one of the asymptotic solutions of the conjugate problem. In solving the conjugate problems, the asymptotic solutions have a significant role in testing the accuracy of numerical algorithms.

Heat and binary mass transfer from a sphere with uniform temperature/concentration was studied in [2,10–13]. The aim of this paper is to analyse the multicomponent (ternary) mass transfer from a sphere with uniform concentrations. Being the first article dedicated to this subject, we will focus on the specific problems of the multicomponent mass transfer. The principal aspect investigated is the influence of the cross-diffusion coefficients on the mass transfer rate at different values of Henry numbers and self-diffusivity ratio. We restrict our analysis to rigid spheres in creeping flow and moderate Peclet numbers (*Pe* on the order 100).

2. Basic equations

Let us consider a multicomponent sphere of diameter d (considerably higher than the molecular mean free path of the surrounding fluid) and a rigid surface placed in a vertical flow of an incompressible, Newtonian fluid having free stream velocity U_∞ (see Fig. 1). Oscillations and rotation of the sphere do not occur during the movement. The solutions are dilute so that the flow and mass transfer are uncoupled (the effects of solute buoyancy are negligible). The sphere Reynolds number is assumed considerably small compared to unity (creeping flow) and the flow is steady and axisymmetric. Due to the complexity of the problem, the following supplementary assumptions are considered:

(i) during the mass transfer, the volume and the shape of the sphere remain constant;
(ii) the physical properties are constant;
(iii) no phase change occurs during the mass transfer;
(iv) the system is isothermal;
(v) the only diffusion mechanism is the Fick diffusion mechanism;
(vi) at the interface, thermodynamic equilibrium is established instantaneously.

In a mixture of n components, only $n-1$ concentrations and mass fluxes are linearly independent. Therefore, only $n-1$ mass balance equations need to be written for an n-species multicomponent system.

The assumption of constant diffusion coefficients is known as "*linearized theory*", [7,14–16]. It must be mentioned that the idea to consider constant, average values for the physical properties in heat/mass transport equations is considerably older than [14–16] (for example, see [17]).

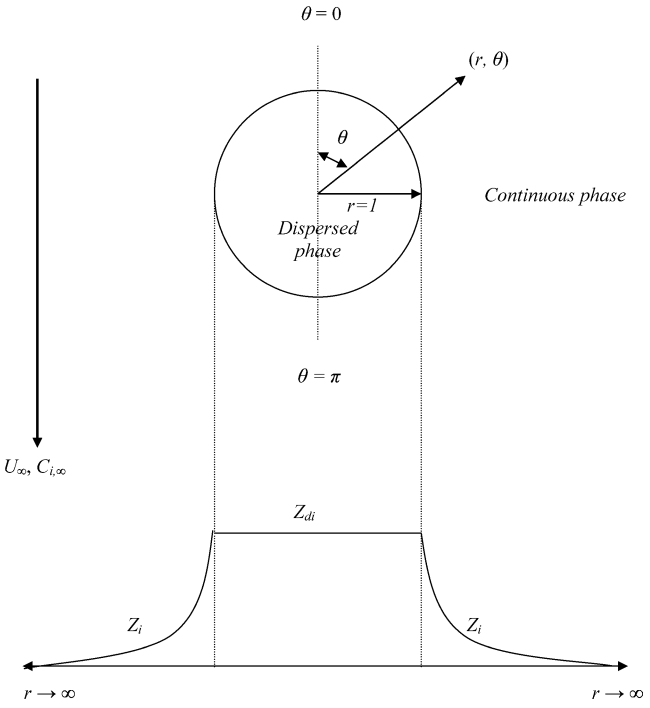

Fig. 1. Schematic of the problem.

As a consequence of assumption (vi), the dispersed and continuous phase concentrations C_{di} and C_i, $i = 1, \ldots, n-1$, at the interface are related by the expression

$$\mathbf{C_d}|_{r'=d/2} = \mathbf{HC}|_{r'=d/2}$$

where $\mathbf{H}$ is the $n-1 \times n-1$ Henry number matrix, $\mathbf{C_d}$ the $(n-1)$-dimensional vector of dispersed phase concentrations and $\mathbf{C}$ the $(n-1)$-dimensional vector of continuous phase concentrations. The elements of Henry number matrix, H_{ij}, are defined by:

$$H_{ij} = \frac{\partial C_{di}}{\partial C_j}$$

The elements of $\mathbf{H}$ depend on concentrations. For dilute solutions, $\mathbf{H}$ may be considered constant and calculated at average concentration values. Also, in this work, the off-diagonal terms of the Henry numbers matrix are considered negligible in comparison with the diagonal terms. This assumption is not too bad for dilute solutions. It is usually valid for ideal solutions.

Under these assumptions, the governing nondimensional equations, expressing conservation of chemical species, in spherical coordinates (r, θ) are:

$$\frac{\partial Z_i}{\partial \tau} + \frac{Pe}{2}\left(V_R \frac{\partial Z_i}{\partial r} + \frac{V_\theta}{r}\frac{\partial Z_i}{\partial \theta}\right) = \sum_{j=1}^{n-1} D_{ij}\gamma_{ij}\left[\frac{1}{r^2}\frac{\partial}{\partial r}\left(r^2\frac{\partial Z_j}{\partial r}\right) + \frac{1}{r^2\sin\theta}\frac{\partial}{\partial \theta}\left(\sin\theta\frac{\partial Z_j}{\partial \theta}\right)\right] \quad i = 1, \ldots, n-1 \tag{1a}$$

$$\frac{\mathrm{d}Z_{di}}{\mathrm{d}\tau} = \frac{3}{2H_{ii}}\int_0^\pi \sum_{j=1}^{n-1} D_{ij}\gamma_{ij}\frac{\partial Z_j}{\partial r}\Big|_{r=1}\sin\theta\,\mathrm{d}\theta \quad i = 1, \ldots, n-1 \tag{1b}$$

The dimensionless variables and groups of the governing equations are:

$$r = 2r'/d, \qquad \tau = 4t\text{Đ}_{11}/d^2, \qquad D_{ij} = \text{Đ}_{ij}/\text{Đ}_{11}$$

$$Z_i = \frac{C_i - C_{i,\infty}}{C_{di,0}/H_{ii} - C_{i,\infty}}$$

$$Z_{di} = \frac{C_{di} - H_{ii}C_{i,\infty}}{C_{di,0} - H_{ii}C_{i,\infty}}$$

$$\gamma_{ij} = \frac{C_{dj,0}/H_{jj} - C_{j,\infty}}{C_{di,0}/H_{ii} - C_{i,\infty}}$$

$$Pe = U_\infty d/\text{Đ}_{11},$$

where r' is the radial coordinate in spherical coordinate system, Đ_{ij} are the Fickean diffusion coefficients of the transferring species and C_i and C_{di} respectively are the mass concentration of the transferring species in the continuous and dispersed phases. The continuous phase Peclet number, Pe, and the Fourier number (nondimensional time variable), τ, were defined considering the self-diffusion coefficient Đ_{11} as the reference diffusion coefficient. The nondimensional velocity components are those derived by Stokes and given by the expressions [1,4]:

$$V_R = -\left(1 - \frac{3}{2r} + \frac{1}{2r^3}\right)\cos\theta$$

$$V_\theta = \left(1 - \frac{3}{4r} - \frac{1}{4r^3}\right)\sin\theta$$

The boundary conditions to be satisfied are:

- interface ($r = 1$)

$$Z_i = Z_{di}, \quad i = 1, \ldots, n-1 \tag{2a}$$

- free stream ($r = \infty$)

$$Z_i = 0, \quad i = 1, \ldots, n-1 \tag{2b}$$

- symmetry axis ($\theta = 0, \pi$)

$$\frac{\partial Z_i}{\partial \theta} = 0, \quad i = 1, \ldots, n-1 \tag{2c}$$

The dimensionless initial conditions are:

$$\tau = 0, \qquad Z_{di} = 1, \quad Z_i(r > 1) = 0, \quad i = 1, \ldots, n-1 \tag{3}$$

The quantities of interest used to characterize the mass transfer from a sphere are: (1) sphere dimensionless concentrations Z_{di}, and (2) overall instantaneous Sherwood numbers, **Sh**. The elements of the Sherwood number matrix (dimensionless mass transfer coefficients), Sh_{ij}, are defined by:

$$Sh_{ij} = k_{ij}d/\text{Đ}_{11}$$

where k_{ij} are the elements of the mass transfer coefficients matrix. The mass transfer coefficients k_{ij} are defined as follows:

$$\sum_{j=1}^{n-1}\frac{1}{2}\int_0^{\pi}-Đ_{ij}\frac{\partial C_j}{\partial r'}\Big|_{r'=d/2}\sin\theta\,\mathrm{d}\theta = \sum_{j=1}^{n-1}k_{ij}(C_j|_{r'=d/2}-C_{j,\infty}),\quad i=1,\ldots,n-1$$

The dimensionless version of the previous relation is:

$$\sum_{j=1}^{n-1}\int_0^{\pi}-D_{ij}\gamma_{ij}\frac{\partial \mathbf{Z}_j}{\partial \mathbf{r}}\Big|_{\mathbf{r}=1}\sin\theta\,\mathbf{d}\theta = \sum_{j=1}^{n-1}\mathbf{Sh}_{ij}\gamma_{ij}\mathbf{Z}_j|_{\mathbf{r}=1},\quad i=1,\ldots,n-1$$

Note that in the previous relations, due to the assumptions of thermodynamic equilibrium at interface and uniform concentrations inside the sphere, $C_j|_{r'=d/2}$ and $Z_j|_{r=1}$ are independent of the angular coordinate θ.

The dispersed phase concentrations Z_{di} are quantities that do not require any supplementary comments. However, the evaluation of the *Sh* numbers in multicomponent mass transfer systems deserves supplementary explanations.

In almost all situations, multicomponent mass transfer problems have been solved based on the methodology developed by Toor [14,15] and Stewart and Prober [16]. Similar ideas were used in solving other cross-diffusion phenomena [18], although articles that do not follow this particular method are [19–21]. We will not discuss the technique in detail here. It is well presented in [7,14–16]. The principal steps are (we refer to the general case):

- the original set of equations is transformed into a set of $n-1$ independent (uncoupled) binary diffusion problems; the transformation consists of multiplying the mathematical model by the modal matrix $\mathbf{P}^{-1}$ of the matrix of diffusion coefficients and inserting the identity matrix $\mathbf{P}\mathbf{P}^{-1}$ between the diffusion coefficients matrix and the diffusion mass fluxes (**P** is the matrix of right eigenvectors of the diffusion coefficient matrix); the original variables transform into new ones, named pseudo-concentrations, while the velocity field remains unchanged;
- solution of the transformed problem;
- calculation of the multicomponent solution by the inverse transformation (the pseudo-variables are multiplied by **P**).

Obviously, this algorithm works if the diffusion coefficients matrix is a nondefective matrix [22]. For brevity, according to [15,16], this method is referred to here as the *matrix method* (MM).

Unfortunately, when we apply MM to the present mathematical model, the system (1b) can be uncoupled only if $H_{11}=H_{22}$. Under any other conditions, the standard MM procedures to define and calculate the multicomponent Sherwood number matrix (the so-called "*matrix generalization of binary functions*" [16]) cannot be followed in this work.

We consider that the multicomponent Sherwood number matrix, **Sh**, is defined by the dimensionless mass balance equation of the sphere, i.e.,

$$\frac{\mathbf{d}\mathbf{Z}_d}{\mathbf{d}\tau}=-\frac{3}{2}\mathbf{H}^{-1}\widehat{\mathbf{Sh}}\mathbf{Z}_d \tag{4}$$

where $\widehat{\mathbf{Sh}}$ is the matrix with elements $\widehat{Sh}_{ij}=Sh_{ij}\gamma_{ij}$, $\mathbf{Z}_d$ is the vector of dispersed phase concentrations and $\mathbf{H}^{-1}$ is the inverse of the Henry numbers matrix assumed diagonal. The driving force is the difference between the sphere's concentration and the concentration far from the sphere. Note that the boundary condition (2a) and the definition of **Sh** should be taken into consideration to check the consistency of (4) with (1b).

There are many ways to calculate $\widehat{\mathbf{Sh}}$ defined by (4). As example, we assume that the numerical values of $\mathbf{Z}_d$ and $\mathrm{d}\mathbf{Z}_d/\mathrm{d}\tau$ are known. After some elementary algebraic manipulations, we obtain

$$\widehat{\mathbf{Sh}}=-\frac{2}{3}\mathbf{H}\left(\frac{\mathbf{d}\mathbf{Z}_d}{\mathbf{d}\tau}\otimes\mathbf{Z}_d^{\mathrm{T}}\right)\left(\mathbf{Z}_d\otimes\mathbf{Z}_d^{\mathrm{T}}\right)^{-1} \tag{5}$$

where the symbol $\otimes$ refers to the outer (dyadic) product and the superscript T indicates the transpose. Relation (5) should not be viewed as an analytical development of relation (4). It represents only a problem of numerical calculus. **Sh** can be also calculated from the pseudo-variables of MM.

For the process analysed in this work, the quantities of first interest are the dispersed phase concentrations. In *binary* mass transfer the instantaneous overall *Sh* number receives the same attention as Z_d for the following reasons:

- in almost all situations *Sh* tends to a frozen asymptotic value;
- a frozen asymptotic *Sh* value allows a quick and easy estimation of the dispersed phase concentration (from the sphere's mass balance equation—the scalar equivalent of (4)).

Thus, the asymptotic *Sh* values represent a simple (albeit artificial) way to describe the asymptotic behaviour of the system. For multicomponent mass transfer systems however, the estimation of Z_{di} from asymptotic $\widehat{\mathbf{Sh}}$ is not an elementary computation (in comparison with the binary mass transfer).

3. Method of solution

The radial coordinate r was replaced by x through the transformation $r=\exp x$. As a result, the use of a constant

discretization parameter for x made it possible to obtain a more dense mesh near the sphere surface, where the gradients are large and where an accurate numerical approximation is needed. The external boundary condition is assumed to be valid at a large but finite distance, r_∞, from the center of the sphere.

Two methods were used to solve the mathematical model: the solution of (1)–(3) in its original form and MM (when MM may be used, of course). In both cases, the mathematical model is a system formed by 2D parabolic partial differential equations (PDE) that describe the mass transfer in the continuous phase and ordinary differential equations (ODE) that describe the mass balance of the sphere. The finite difference method was used for spatial discretization (the exponentially fitted scheme [23]) of the parabolic PDE. The spatial meshes have 129×129 and 257×257 points. The discretized parabolic equations were solved by a splitting method. The difference between the two methods consists in the nature of the discrete spatial operator splitting. A standard splitting [24], was used for MM. The splitting procedure described in [25] is used to solve (1)–(3) in the original form. The ODE were integrated by an explicit modified Euler algorithm. The integral from relation (1b) was calculated by the Simpson's 3/8 rule [26]. The time step was variable and changed from the start of the computation to the final stage. The initial and final values of the time step depend on the parameter values.

4. Results

The model of the sphere with rigid surface is usually assumed to represent a solid particle in a fluid environment. However, a contaminant present in a fluid–fluid system can eliminate the internal circulation [1]. In most systems of practical importance it is very difficult to remove entirely surface-active contaminants. Under these conditions, even some fluid–fluid disperse systems can be modelled quite well by a sphere with a rigid surface.

The present computations were restricted to the case of ternary systems, i.e., $n = 3$. For a ternary system, the mathematical model (1)–(3) contains seven independent dimensionless parameters: D_{12}, D_{21}, D_{22}, H_{11}, H_{22}, Pe and γ_{12} (or γ_{21}). Pe takes only one value, $Pe = 100$, because its influence on the mass transfer is easy to foresee (the increase in Pe increases the mass transfer rate and diminishes the wake phenomena, if these phenomena are present). The Henry numbers, H_{11} and H_{22}, vary in the range $[0.01, 100]$. Without loss of generality, we assume $\gamma_{12} = \gamma_{21} = 1.0$ as γ_{ij} always appears multiplied by D_{ij} in Eq. (1). Values of the normalized self-diffusion coefficient D_{22} (the self-diffusivity ratio) between $[0.1, 10.0]$ cover the realistic situations considered in this paper.

The key parameters of this work are the normalized cross-diffusion coefficients. Two rules must be taken into consideration when the values of the cross-diffusion coefficients are chosen [7]. The first establishes that the diffusion coefficient matrix is a positive definite one. The second states that the self-diffusion coefficients (in the transformed MM system) are positive quantities. Based on these rules, D_{12} and D_{21} take positive or negative values such that:

$$D_{22} - D_{12}D_{21} > 0 \tag{6a}$$

$$(1 - D_{22})^2 + 4D_{12}D_{21} \geqslant 0 \tag{6b}$$

Remember that D_{11} is unity by definition.

The first task in any numerical work is to validate the code's ability to reproduce published results accurately. Unfortunately, there are no data in the literature to verify the accuracy of the present computations. Two accuracy tests were used in this work: (1) the comparison between the solutions provided by the two methods used; (2) the simulation of the cases when the mathematical model is equivalent to a single equation (as for example, $D_{12} = D_{21}$, $D_{22} = 1$, $H_{11} = H_{22}$). The results obtained showed that the relative errors between the solutions provided by different methods are smaller than 1%.

Even with restrictions (6), D_{12} and D_{21} can potentially take values on a relatively large domain. Assuming the dependence Z_{di} versus D_{ij} to be monotone, we think that the influence of D_{ij} on Z_{di} is best emphasized by its solutions for extremal cases (even when the extremal cases refer to hypothetical situations) and their value relative to the binary diffusion solution. If, for example, $|D_{12}| \geqslant |D_{21}|$ and the other parameters are constants, the boundary solutions for Z_{d1} are given by the following normalized diffusion coefficients matrices:

$$\begin{bmatrix} 1 & D_{12} \\ 0 & D_{22} \end{bmatrix}, \qquad \begin{bmatrix} 1 & D_{12} \\ D_{12} & D_{22} \end{bmatrix}$$

(if D_{12} and D_{21} have the same sign)

or

$$\begin{bmatrix} 1 & D_{12} \\ 0 & D_{22} \end{bmatrix}, \qquad \begin{bmatrix} 1 & D_{12} \\ -D_{12} & D_{22} \end{bmatrix}$$

(if D_{12} and D_{21} have different signs)

4.1. Simple solutions

The influence of the cross-diffusion coefficients on the mass transfer rate is analysed step by step, starting with the simplest situations. The investigation begins with the case $D_{22} = 1$ and $H_{11} = H_{22}$. From the simulations made, we present those plotted in Fig. 2. We considered that this choice captures the salient features encountered during the numerical experiments. If $D_{22} = 1$ and $H_{11} = H_{22}$, the solution exhibits the following symmetry property: the interchange of the cross-diffusion coefficient values leads to the interchange of dimensionless concentrations values. For this reason, only Z_{d1} is depicted in Fig. 2. When $D_{22} = 1$, relation (7b) imposes the same sign for both cross-diffusion coefficients.

Based on extensive numerical experiments and the results plotted in Fig. 2, we can note the following facts:

- as expected for both species diffusing outwards, positive values of the cross-diffusion coefficients increases the mass transfer rate while negative values decreases it (Fig. 2(a));
- the influence of cross-diffusion becomes significant when the ratio (cross-diffusion coefficient)/(self-diffusion coefficient) is $O(10^{-1})$ (Fig. 2(b), (c));
- if $|D_{12}|$ exceeds $|D_{21}|$, the variation of D_{21} in the range $[0, D_{12}]$ does not influence significantly the mass transfer of Z_{d1} (Fig. 2(b));
- if $|D_{21}|$ exceeds $|D_{12}|$, the variation of D_{12} in the range $[0, D_{21}]$ influences significantly the mass transfer of Z_{d1} (Fig. 2(c));
- the previous observations are valid for any values of the Henry number.

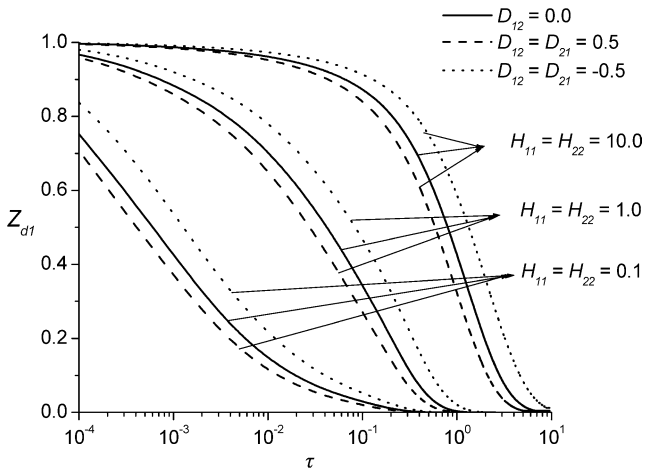

(a)

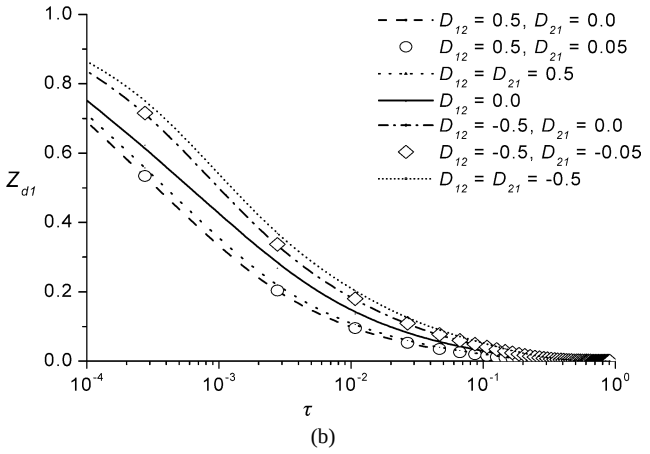

(b)

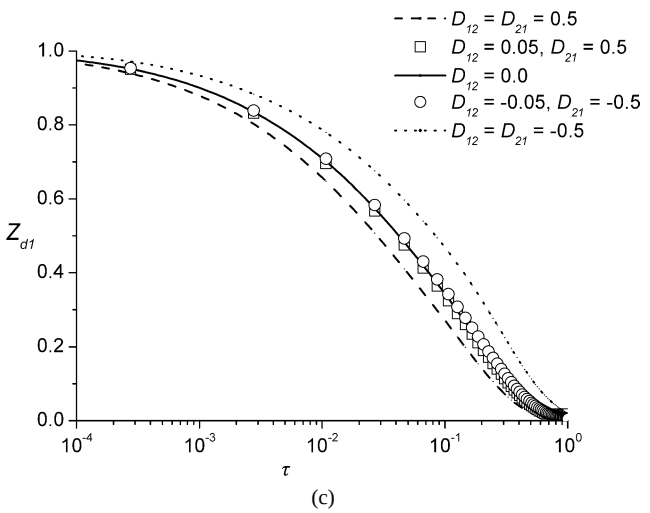

(c)

Fig. 2. Variation of the sphere concentration Z_{d1} with dimensionless time at $D_{22} = 1.0$ and different Henry numbers values; (a) $D_{12} = D_{21}$; (b) $H_{11} = H_{22} = 0.10$; (c) $H_{11} = H_{22} = 1.0$.

The numerical experiments revealed an interesting aspect (relatively hard to detect from Fig. 2) that deserves to be discussed. For positive values of the cross-diffusion coefficients, in the final stage of the process (i.e., when $Z_{d1} \to 0$), the interface mass flux, and implicitly the time variation of Z_{d1}, computed when $D_{12} \neq D_{21}$ differs significantly from that calculated when $D_{12} = D_{21}$ or $D_{12} = 0$ (binary diffusion) (see Fig. 3). Obviously, when $D_{12} \neq D_{21}$, the mass transfer rate of the two species are different. One evolves faster (for example component 1) while the other (component 2) slower. At small values of dispersed phase concentrations of component 1 ($Z_{d1} < 0.1$), one expects the self-diffusion flux to become smaller than the cross-diffusion flux. This is not an unrealistic phenomenon. The problem is: when Z_{d1} is small and considerably smaller than Z_{d2}, does the cross-diffusion flux calculated with a constant D_{12} value overestimate or not the real mass transfer rate? For example, if we perform a blind numerical integration, we reach the situation when there exists a finite, positive mass flux for Z_1 at the interface while the sphere is lacking component 1. A careful examination of the data showed that, independent of the method used, numerical errors do not play any role in this situation. Note that when MM is applied, we solve effectively a binary diffusion problem: for a binary diffusion

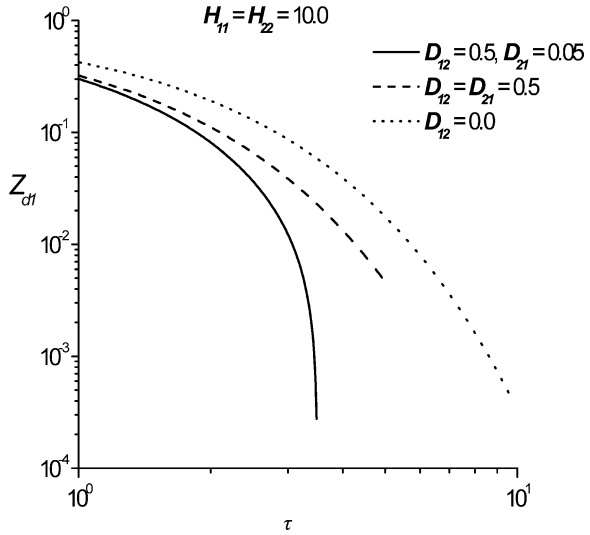

Fig. 3. Final time evolution of dispersed phase concentration Z_{d1} at $D_{22} = 1.0$ and $H_{11} = H_{22} = 10.0$.

problem, it is not difficult to evaluate the accuracy of the numerical solution.

Our opinion is that constant values of the cross-diffusion coefficients overestimate the mass transfer rate in this situation. In reality, the diffusion coefficients depend on the species concentration. Also, the mass flux should tend to zero when the concentrations tend to zero. In almost all cases analysed until now, the diffusion coefficients were assumed constants, independent of the concentrations. In the case of binary diffusion, the system self-regulates. The decrease in the transferring species concentration implies a similar decrease in the mass flux. By contrast, in the case of ternary systems, the control by mass fluxes (assuming constant diffusivity) does not work in every situation.

For negative values of the cross-diffusion coefficients, a similar discussion may take place by replacing in the previous paragraphs the word *overestimate* by *underestimate*. Based on a careful examination of the numerical data, we consider that even for negative values of the cross-diffusion coefficients the system cannot self-regulate as in the case of binary diffusion. The uncertainty about the final diffusion rate persists. However, in this case it is easier to control the system's evolution.

The previous discussions raise the following issues: (1) the confidence in the asymptotic *Sh* values (i.e., dimensionless mass transport rates); (2) the confidence in the data referring to phenomena occurring on the sphere surface (osmotic diffusion, diffusion barrier and reverse diffusion, all to be described in more detail later). The overall instantaneous *Sh* numbers tend to a frozen asymptotic value and also osmotic diffusion, diffusion barrier and reverse diffusion phenomena occur on the sphere surface when $Z_{di} < 0.1$. Their accurate computation depends on the accuracy of the mass transfer rate computation at small Z_{di} values.

Similar discussions could take place for any new set of parameters used in this work. To avoid repetition, we will not touch this problem in the remainder of this section. This does not mean however that these problems disappear or we have removed all uncertainties.

4.2. Further solutions

The next simulations were made assuming: (1) $D_{22} = 1$, $H_{22} \neq H_{11} = 1$ and (2) $D_{22} \neq 1$, $H_{11} = H_{22} = 1$. In the first case, the cross-diffusion coefficients must have the same sign because $D_{22} = 1$. In case (2), D_{12} and D_{21} can have op-

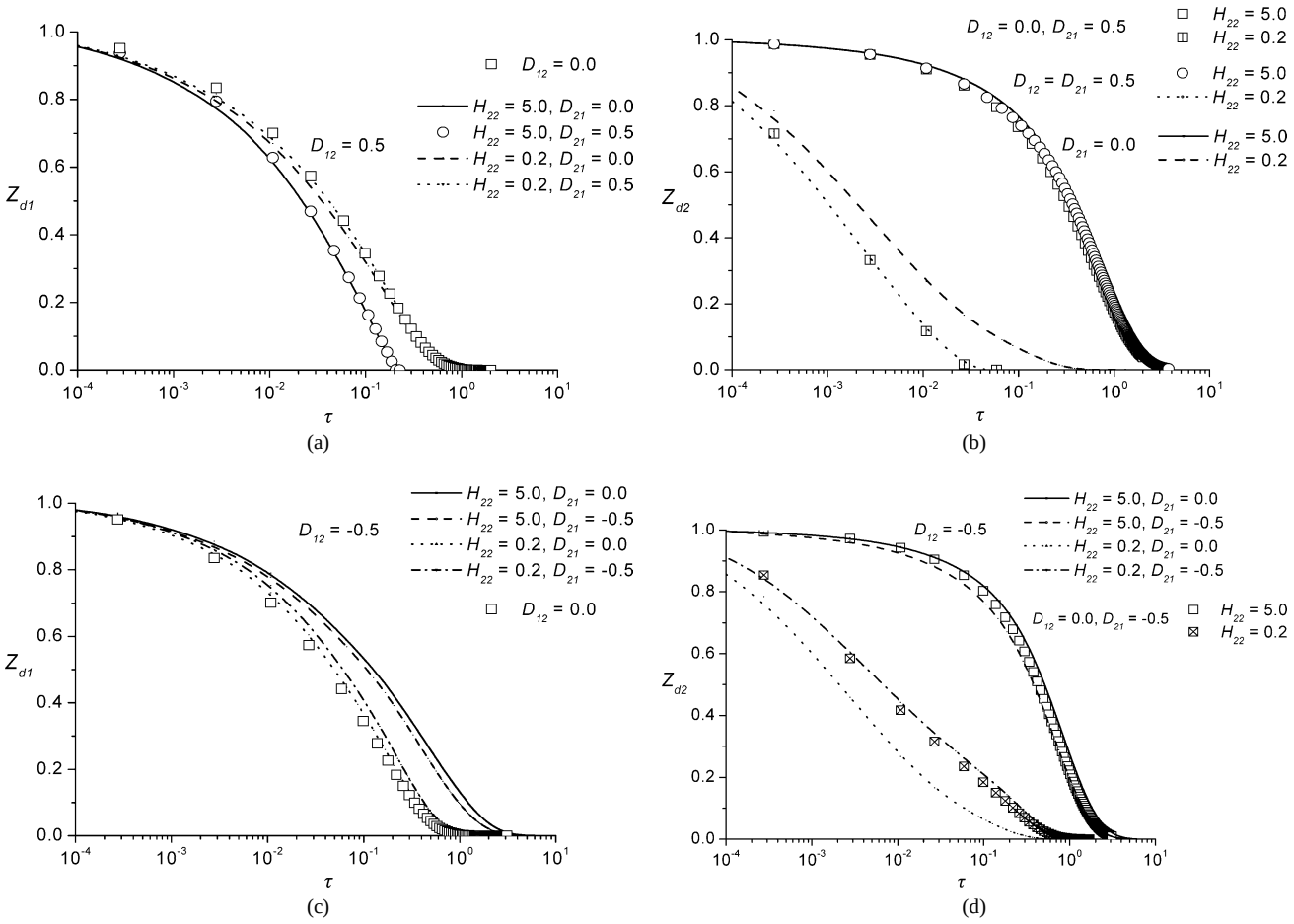

Fig. 4. Time evolution of dispersed phase concentrations Z_{d1} and Z_{d2} at $D_{22} = 1.0$, $H_{11} = 1.0$ and $H_{22} \neq H_{11}$.

posite signs. In both cases a clear distinction between Z_{d1} and Z_{d2} occurs.

Fig. 4 show the influence of H_{22} on the mass transfer rates. If the cross-diffusion coefficients are positive, we observe the following aspects (Fig. 4(a), (b)):

- if $H_{22} > 1$, the mass transfer of component 1 is considerably accelerated; D_{21} does not influence Z_{d1} in practice; after the disappearance of species 1, the mass transfer of component 2 unfolds as a binary diffusion;
- when $H_{22} < 1$, Z_{d1} and Z_{d2} interchange their roles.

For negative values of D_{12} and D_{21} (Fig. 4(c), (d)), the cross-diffusion influences significantly the mass transfer of component 1 if $H_{22} > 1$ and the mass transfer of component 2 for $H_{22} < 1$. When $H_{22} > 1$, the time evolution of Z_{d2} is similar to that predicted by binary diffusion when both Z_{d1} and Z_{d2} tend to zero. When $H_{22} < 1$, the time evolution of Z_{d1} is similar to that predicted by binary diffusion.

Fig. 5(a), (b) show that if D_{22} takes values greater than one (e.g., $D_{22} = 5.0$) and $H_{11} = H_{22} = 1$, the impact of cross-diffusion decreases for both species. We observe that there are two groups of curves. Each group has in effect only three curves; one corresponding to D_{12} $(D_{21}) = 0.5$, one describing the binary diffusion and one for D_{12} $(D_{21}) = -0.5$. If D_{22} increases, the mass transfer at the interface for component 2 increases. Thus, component 1 becomes the *dominant species* and a strong influence of cross-diffusion on component 2 is expected. However, the increase in D_{22} simultaneously maintaining D_{21} at the same level, leads to a decrease in the cross-diffusion weight. These two facts that act in opposition lead to the situation plotted in Fig. 5(a), (b). It must be mentioned that the cases when the cross-diffusion coefficients have opposite signs do not exhibit a distinct behaviour.

If $D_{22} < 1$ and $H_{11} = H_{22} = 1$, component 2 becomes the *dominant species* (Fig. 5(c), (d)), surviving longer than component 1. The mass transfer of component 1 depends effectively only on D_{12} values. Before the disappearance of component 1, we observe a relative spread in Z_{d2} curves, thus a stronger influence of the cross-diffusion D_{21}. Negative values of D_{12} maintain Z_{d1} a longer time in the system

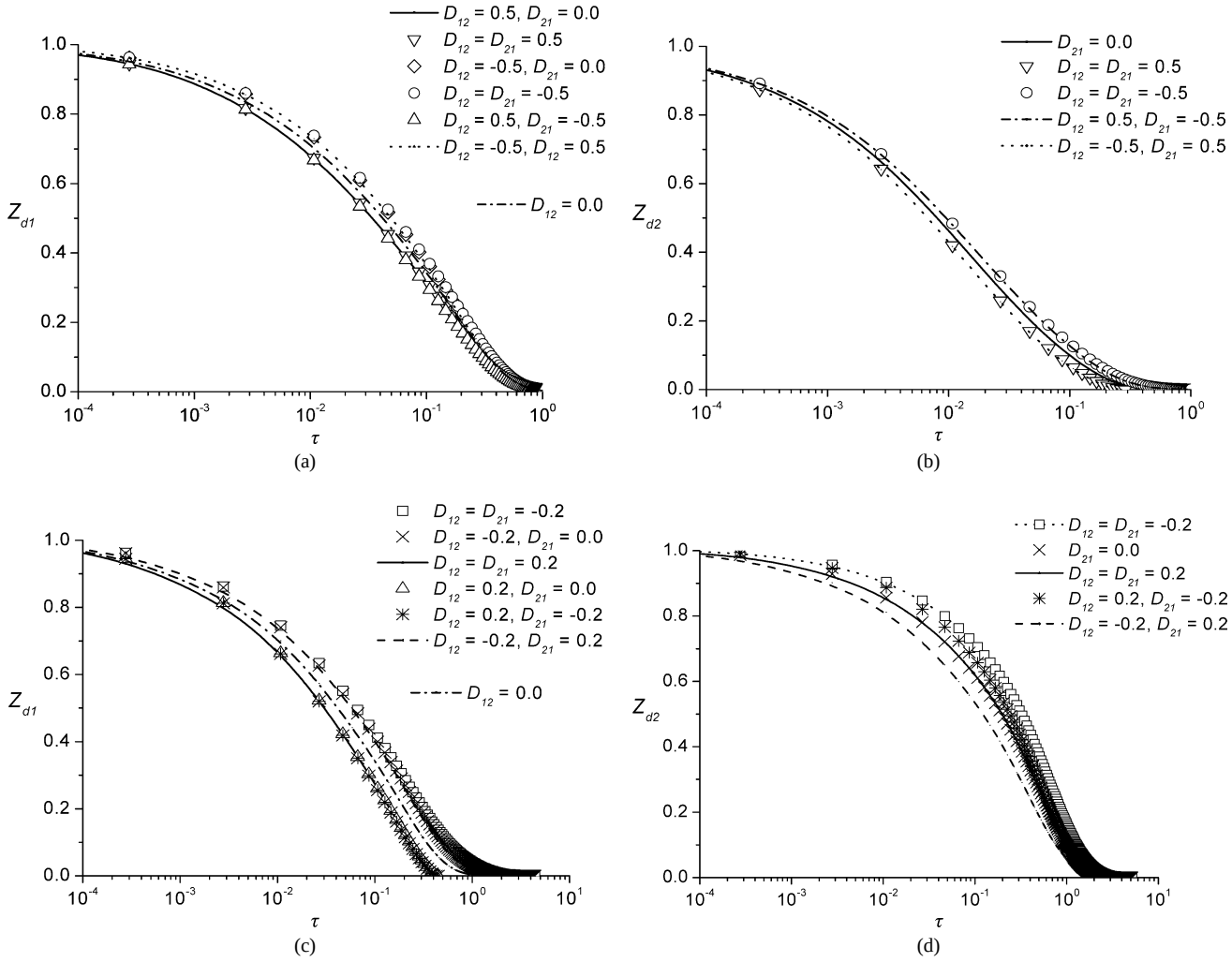

Fig. 5. Time variation of the sphere concentrations Z_{d1} and Z_{d2} at $H_{11} = H_{22} = 1.0$ and $D_{22} \neq 1.0$; (a), (b) $D_{22} = 5.0$; (c), (d) $D_{22} = 0.20$.

and implicitly generate a higher influence of cross-diffusion on Z_{d2}. After the disappearance of component 1, the Z_{d2} curves converge to the binary diffusion solution.

In the final step of the present investigation, we simulated the situations when $D_{22} \neq 1$ and $H_{22} \neq H = 1$. The values of D_{22} and H_{22} to simulate may be selected in two ways: (a) the effects of D_{22} and H_{22} act in the same direction or (b) D_{22} and H_{22} have opposite effects. We chose option (b), because we considered it much more interesting.

Even when D_{22} and H_{22} act in opposition, it is expected that one of these parameters will become dominant. The problem of interest in this context is whether the time evolution of the dispersed phase concentrations is dictated only by D_{22} and H_{22} or, for a given set of D_{22} and H_{22} values,

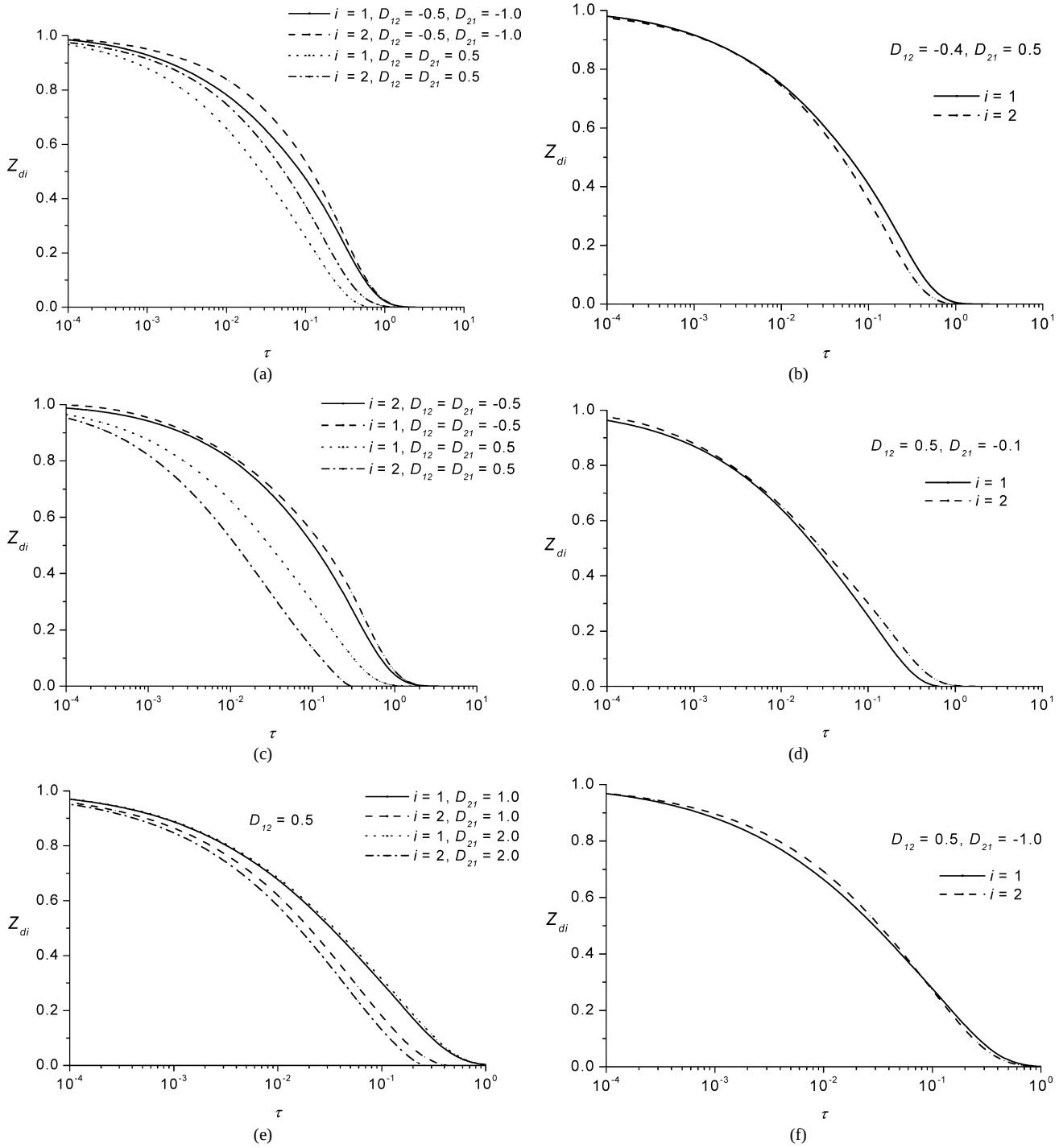

Fig. 6. Sphere concentrations Z_{d1} and Z_{d2} as function of dimensionless time; $H_{11} = 1.0$; (a), (b) $D_{22} = H_{22} = 2.0$; (c), (d) $D_{22} = H_{22} = 0.50$; (e), (f) $D_{22} = 5.0$, $H_{22} = 2.0$.

whether the cross-diffusion coefficients can compensate the combined action of D_{22} and H_{22}.

The data plotted in Fig. 6 lead to the following observations:

- for $D_{22} = H_{22} > 1$ (Fig. 6(a)) or $D_{22} = H_{22} < 1$ (Fig. 6(c)) and $D_{12} = D_{21} > (<)\ 0$, the influence of H_{22} is stronger than that of D_{22}; the time evolution of Z_{di} is similar to that observed in Fig. 4;
- increasing D_{22}, (Fig. 6(e)) the influence of self-diffusivity ratio exceeds that of H_{22} for positive values of cross-diffusion coefficients; the time evolution of dispersed phase concentrations resemblances that encountered in Fig. 5(a), (b);
- for all situations, the case $D_{12} < 0$, $D_{21} > 0$ exhibits distinct and interesting characteristics; the cross-diffusion coefficients can counterbalance the resultant of D_{22} and H_{22} effects; for example, in Fig. 6(a) the component 2 is the dominant species while in Fig. 6(b) component 1 becomes the dominant species; however, it is difficult to give a final verdict in this case; for the curves plotted in Fig. 6, the difference between H_{11} and H_{22} is not great.

4.3. Asymptotic values of Sh

The numerical experiments performed in this work revealed two general situations. In the first, there is a significant difference between the sphere depletion times of the two species. In the second, the depletion time of the two species is approximately the same. We think that asymptotic values of the *Sh* numbers describe better the asymptotic behaviour of the system in the second situation.

Table 1 present some of the asymptotic *Sh* values calculated in this work. The overall instantaneous *Sh* number was calculated by Eq. (5) at each time integration step (since $\gamma_{ij} = 1$ in the computations, $\mathbf{Sh} = \widehat{\mathbf{Sh}}$). When $H_{11} = H_{22}$, the *Sh* values computed with Eq. (5) were compared to those calculated with the standard MM methodology. The agreement was very good (the relative errors are smaller than 1%). For the cases presented in Table 1, the overall instantaneous *Sh* numbers tend to a frozen asymptotic value when both species are present in system.

We tried by this selection to set off the influence of different parameters on **Sh**. Based on the data depicted in Table 1, we can make the following observations:

- the variation in D_{12} (D_{21}) influences significantly only Sh_{12} (Sh_{21}) (Table 1(a));
- the variation of D_{22} influences Sh_{22}, Sh_{12} and Sh_{21} (Table 1(b));
- if $H_{22} > H_{11}$, the variation of H_{22} influences significantly Sh_{11}, Sh_{12} and Sh_{22} (Table 1(c)).

Table 1(a)
Asymptotic values of **Sh**; $H_{11} = H_{22} = 1.0$; $D_{22} = 2.0$

H_{11}	H_{22}	D_{22}	D_{21}	D_{12}	Sh_{11}	Sh_{12}	Sh_{21}	Sh_{22}
1	1	2	−0.5	0.4	3.48	0.58	−0.73	4.94
1	1	2	−0.5	0.2	3.45	0.29	−0.73	4.91
1	1	2	−0.5	0.1	3.43	0.18	−0.74	4.90
1	1	2	−0.5	−0.1	3.39	−0.15	−0.74	4.87
1	1	2	−0.5	−0.3	3.35	−0.45	−0.73	4.84
1	1	2	−0.5	−0.5	3.31	−0.75	−0.75	4.81
1	1	2	−0.3	−0.5	3.35	−0.75	−0.45	4.84
1	1	2	−0.1	−0.5	3.39	−0.74	−0.15	4.87

Table 1(b)
Asymptotic values of **Sh**; $H_{11} = H_{22} = 1.0$; $D_{12} = -0.50$; $D_{21} = -0.10$

H_{11}	H_{22}	D_{22}	D_{21}	D_{12}	Sh_{11}	Sh_{12}	Sh_{21}	Sh_{22}
1	1	0.2	−0.1	−0.5	3.36	−1.33	−0.27	1.24
1	1	0.5	−0.1	−0.5	3.37	−1.12	−0.22	2.26
1	1	1	−0.1	−0.5	3.38	−0.93	−0.19	3.38
1	1	2	−0.1	−0.5	3.39	−0.74	−0.15	4.87
1	1	5	−0.1	−0.5	3.40	−0.48	−0.097	7.26

Table 1(c)
Asymptotic values of **Sh**; $D_{21} = -0.1$, $D_{12} = -0.5$

H_{11}	H_{22}	D_{22}	D_{21}	D_{12}	Sh_{11}	Sh_{12}	Sh_{21}	Sh_{22}
1	2	2	−0.1	−0.5	3.70	−1.53	−0.31	6.76
1	4	2	−0.1	−0.5	4.45	−1.69	−0.34	7.82
1	10	2	−0.1	−0.5	5.1	−1.8	−0.36	8.69
1	10	5	−0.1	−0.5	4.61	−1.52	−0.30	16.77
2	10	5	−0.1	−0.5	4.62	−1.52	−0.30	16.79
0.2	10	5	−0.1	−0.5	4.60	−1.52	−0.30	16.77

4.4. Osmotic diffusion, diffusion barriers and reverse diffusion

Physically unsteady heat/binary mass transfer between a sphere and an ambient flow reveals some unusual aspects. The most important seems to be the thermal/mass wake phenomenon [12,13]. It consists of the local reverse of the transfer direction on the interface in the vicinity of the backward stagnation point. The quantity usually used to describe this phenomenon is the transfer inversion point (TrIP). The TrIP is the point on the sphere surface, measured from the rear stagnation point, where the sign of the local mass flux changes.

In a ternary mass transfer system, similar phenomena are: osmotic diffusion, diffusion barrier and reverse diffusion [27]. Denote by J_{s1}, J_{c1} and $J_1 = J_{s1} + J_{c1}$ the self-diffusion, the cross-diffusion and the total diffusion fluxes of component 1 on the interface, respectively. The osmotic diffusion and the diffusion barrier are defined by (see also Fig. 7):

- $J_{s1} = 0$, $J_1 \neq 0$—osmotic diffusion
- $J_1 = 0$ (with also gradient of composition vanishing)—diffusion barrier.

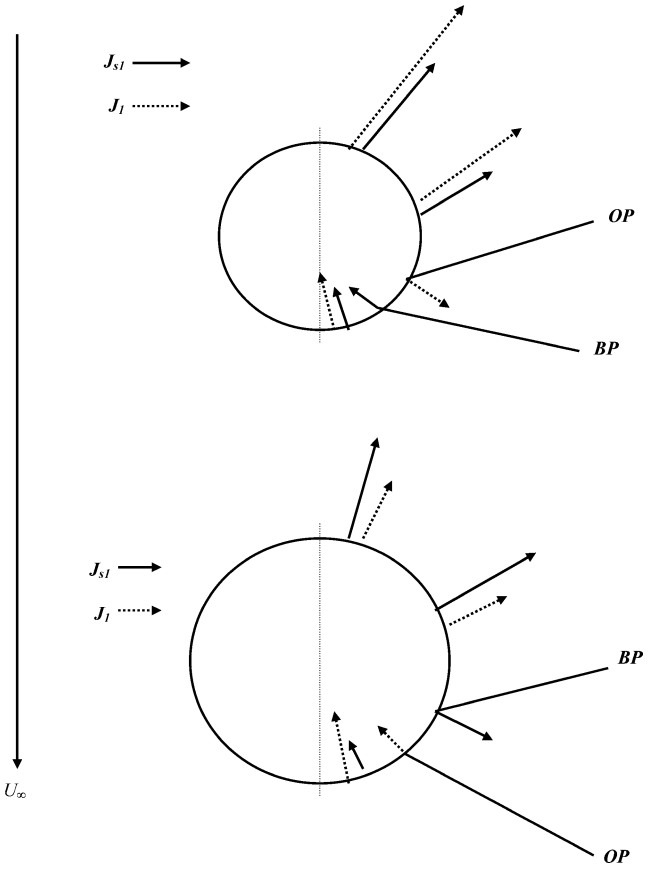

Fig. 7. Schematic of the sphere surface phenomena.

Reverse diffusion refers to the situation when a species diffuses in a direction opposite to that given by its own concentration gradient. Generally, an osmotic diffusion point and a diffusion barrier point delimit the region of reverse diffusion.

The diffusion anomalies that occur on the sphere's surface are quantified in this work by (Fig. 7):

- the osmotic point (OP); the point on the sphere surface, measured from the rear stagnation point, where the self-diffusion flux is equal to zero;
- the barrier point (BP); the point on the sphere surface, measured from the rear stagnation point, where the total diffusion flux is equal to zero.

During the mass transfer process, the OP and BP positions on the sphere surface vary in time until a steady state location is reached.

Toor [27] considers that outside the region of reverse diffusion there exists only normal diffusion. For the present process, normal diffusion exists only in the region delimited by the front stagnation point and OP or BP (depending on which of these points occurs first). Beyond BP or OP, a mass wake phenomenon occurs.

A thorough analysis of these phenomena goes beyond the possibilities of this work. In binary diffusion, TrIP depends only on two parameters: H and Pe. For a multicomponent

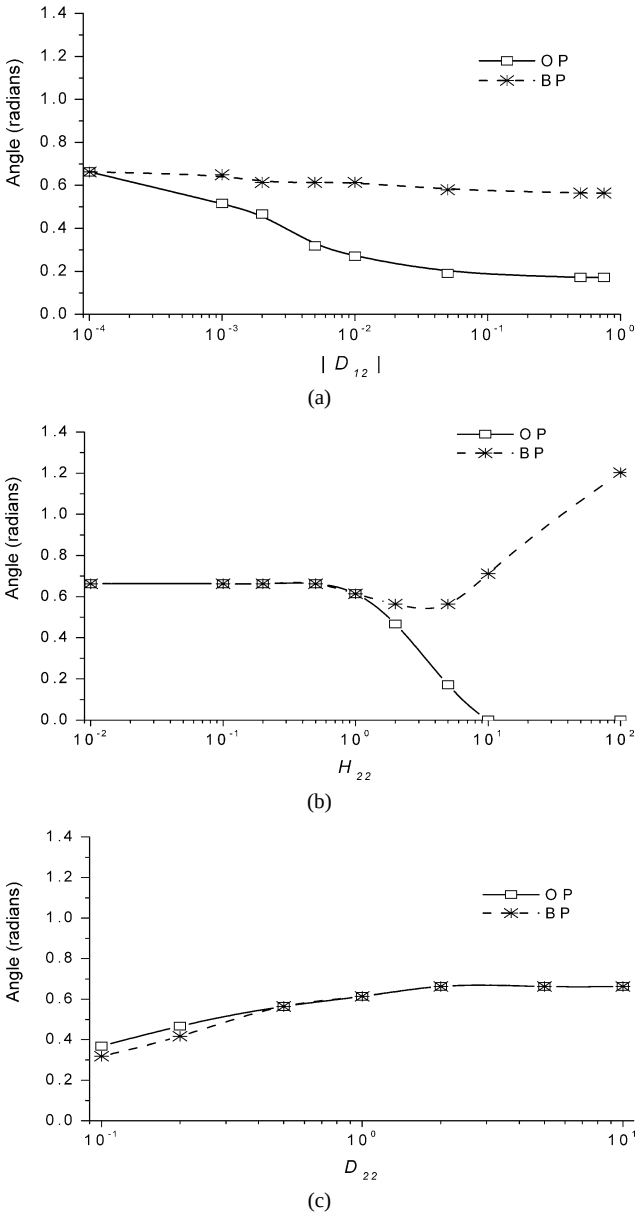

Fig. 8. Steady state position of OP and BP on the sphere surface, measured with respect to the rear stagnation point; $H_{11} = 1.0$ and $D_{21} = 0.0$; (a) $D_{22} = 1.0$; $H_{22} = 5.0$; (b) $D_{22} = 1.0$; $D_{12} = -0.50$; (c) $D_{12} = -0.5$, $H_{22} = 1.0$.

system, OP and BP depend on the Henry number matrix, normalized diffusion coefficient matrix, Pe and γ_{12} (by definition $\gamma_{11} = \gamma_{22} = 1$ and $\gamma_{12}\gamma_{21} = 1$, so only one value is required). In this work we can take only a first step towards analysing this problem. The case chosen to be presented is defined by: $H_{11} = 1$, $D_{21} = 0$ (component 2 participates in the process but it is not influenced by component 1), $D_{12} \in (0, -0.5]$ (for negative values of the cross-diffusion coefficients it is easier to control the system's evolution—see Section 4.1), $D_{22} \in [0.1, 10]$ and $H_{22} \in [0.01, 100]$.

The influence of D_{12}, D_{22} and H_{22} on the steady OP and BP positions is plotted in Fig. 8. Fig. 8(a) shows that D_{12} has a strong influence on OP at even very small values of

D_{12} (values for which the influence of cross-diffusion on mass transfer is not otherwise significant). BP does not vary significantly with D_{12}. When D_{12} begins to affect the mass transfer, OP and BP have a quite stable location. Note that for the case plotted in Fig. 8(a), the mass transfer of component 2 is not affected by the mass wake.

For high values of H_{22}, $H_{22} \geqslant 10$, only BP occurs (Fig. 8(b)). Distinct OP and BP exist for $1 \leqslant H_{22} < 10$. At small H_{22} values, OP and BP coincide and are equal to the binary diffusion TrIP (component 1 is dominant and exhibits essentially binary diffusion). In Fig. 8(a) and (b), OP has smaller values than BP (a normal situation for negative cross-diffusion coefficients). An interesting situation can be viewed in Fig. 8(c). For $D_{22} < 1$, BP has smaller values than OP. At $D_{22} < 1$ and $H_{11} = H_{22} = 1$, the mass transfer of component 1 evolves faster. For component 2, on the sphere surface, a TrIP occurs. This implies negative values of the concentration gradient, $\partial Z_2/\partial r|_{r=1}$, in the vicinity of rear stagnation point. Negative values of the concentration gradient implies positive values of $J_{c1} = D_{12}\partial Z_2/\partial r|_{r=1}$ (because D_{12} is negative) and implicitly $J_1 > J_{s1}$.

5. Conclusions

The objective pursued in this work was to obtain a better understanding of multicomponent mass transfer from a rigid sphere with uniform concentrations in creeping flow. Moderate values of the *Pe* number were assumed. The analysis was directed toward the influence of cross-diffusion on the mass transfer at different values of Henry numbers and self-diffusivity ratio.

The degree of complexity of multicomponent diffusion depends on the problem considered. The numerical results presented in the previous section show that, for the process considered in this work, the multicomponent mass transfer appears as a complex system with its own specific laws. The simple matrix generalization of binary functions cannot catch all salient features of this system. If the ratio cross-diffusion/self-diffusion exceeds $O(10^{-1})$, the present results differ significantly from those provided by binary diffusion. The binary diffusion solutions can be a quite acceptable approximation only for one of the species involved in the process and only at some combinations of parameters values. Constant values of the diffusion coefficients do not estimate fairly the mass transfer rate in the final stage of the process. For a ternary mixture, the system cannot self-regulate by mass fluxes as in the case of binary diffusion.

Acknowledgements

The author would like to express his sincere thanks to the two reviewers for helpful comments and suggestions.

References

[1] R. Clift, J.R. Grace, M.E. Weber, Bubbles, Drops and Particles, Academic Press, New York, 1978.
[2] H. Brauer, Unsteady state mass transfer through the interface of spherical particles—I + II, Internat. J. Heat Mass Transfer 21 (1978) 445–465.
[3] B.I. Brounshtein, V.V. Shegolev, Hydrodynamics, Mass and Heat Transfer in Column Devices, Khimiya, Leningrad, 1988 (in Russian).
[4] S.S. Sadhal, P.S. Ayyaswamy, J.N.-C. Chung, Transport Phenomena with Drops and Bubbles, Springer, Berlin, 1996.
[5] C.F. Curtiss, R.B. Bird, Multicomponent diffusion, Indust. Engrg. Chem. Res. 38 (1999) 2515–2522.
[6] E.D. Negri, W.J. Korchinsky, Multicomponent mass transfer in spherical rigid drops, Chem. Engrg. Sci. 41 (1986) 2401–2406.
[7] R. Taylor, R. Krishna, Multicomponent Mass Transfer, Wiley, New York, 1993.
[8] A.R. Uribe-Ramirez, W.J. Korchinsky, Fundamental theory for prediction of multicomponent mass transfer in single-liquid drops at intermediate Reynolds numbers, Chem. Engrg. Sci. 55 (2000) 3319–3328.
[9] B.I. Brounshtein, A.S. Zheleznyak, G.A. Fishbein, Heat and mass transfer in interactions of spherical drops and gas bubbles with a liquid flow, Internat. J. Heat Mass Transfer 13 (1970) 963–973.
[10] W.Y. Soung, J.T. Sears, Effect of reaction order and convection around gas-bubbles in a gas–liquid reacting system, Chem. Engrg. Sci. 30 (1975) 1353–1356.
[11] E. Ruckenstein, V.-D. Dang, W.N. Gill, Mass transfer with chemical reaction from spherical one or two component bubbles or drops, Chem. Engrg. Sci. 26 (1971) 647–668.
[12] B. Abramzon, C. Elata, Unsteady heat transfer from a single sphere in Stokes flow, Internat. J. Heat Mass Transfer 27 (1984) 687–695.
[13] G. Juncu, Unsteady heat and/or mass transfer from a fluid sphere in creeping flow, Internat. J. Heat Mass Transfer 44 (2001) 2239–2246.
[14] H.L. Toor, Solution of the linearized equations of multicomponent mass transfer: I, AIChE J. 10 (1964) 448–455.
[15] H.L. Toor, Solution of the linearized equations of multicomponent mass transfer: II. Matrix methods, AIChE J. 10 (1964) 460–465.
[16] W.E. Stewart, R. Prober, Matrix calculation of multicomponent mass transfer in isothermal systems, Indust. Engrg. Chem. Fund. 3 (1964) 224–235.
[17] W. Nusselt, Das Grundgesetz des Wärmeüberganges, Gesund. Ing. 38 (42) (1915) 477–482.
[18] Y. Tambour, Transport coupling theory for multicomponent nonequilibrium chemically reacting boundary layers, Phys. Fluids 22 (1979) 1255–1260.
[19] S. van Vaerenbergh, J.C. Legros, Modélisation de la diffusion multiconstituant : l'exemple des systèmes ternaires, Entropie 198/199 (1996) 77–82.
[20] J.P. Larre, J.K. Flatten, G. Chavepeyer, Soret effects in ternary systems heated from below, Internat. J. Heat Mass Transfer 40 (1997) 545–555.
[21] M. Désilets, P. Proulx, G. Soucy, Modelling of multicomponent diffusion in high temperature flows, Internat. J. Heat Mass Transfer 40 (1997) 4273–4278.
[22] G.H. Golub, C.F. van Loan, Matrix Computations, North Oxford Academic, Oxford, 1983.
[23] P.W. Hemker, A numerical study of stiff two-point boundary problems, Ph.D. Thesis, Mathematisch Centrum, Amsterdam, 1977.
[24] G. Marchouk, Méthodes de Calcul Numérique, Mir, Moscow , 1980.
[25] G. Juncu, Splitting-up methods for the numerical solution of multicomponent mass transfer problems, Z. Angew. Math. Mech. (2004), submitted for publication.
[26] C.W. Ueberhuber, Numerical Computations 2: Methods, Software, and Analysis, Springer, Berlin, 1997.
[27] H.L. Toor, Diffusion in three component gas mixtures, AIChE J. 3 (1957) 198–207.